

# Creating a Strong Rain Danger Map for Cyprus

Thomas Krauss<sup>a</sup>, Christodoulos Mettas<sup>b,c</sup>, Josefina Kountouri<sup>b,c</sup>, Constantinos F. Panagiotou<sup>b</sup>, Athanasios V. Argyriou<sup>b</sup>, and Evagoras Evagorou<sup>b</sup>

<sup>a</sup>DLR, Münchener Str. 20, 82234 Wessling, Germany

<sup>b</sup>Eratosthenes Centre of Excellence, Fragklinou Rousbelt 82, 3012 Limassol, Cyprus

<sup>c</sup>Cyprus University of Technology, Arch. Kyprianou 30, 3036 Limassol, Cyprus

## ABSTRACT

In this paper we present a method for creating a strong rain danger map for Cyprus which is based only on terrain information without the need of meteorological and surface type data. The map is a combination of two methods developed at DLR over the past years for prediction of flood dangers from local strong rain events and for dangers from flash floods originating from strong rain events in upstream regions. Beside the explanation of the methods the results are presented and cross-checked with a flood event from 2003 of the Pedaios River south of Nicosia.

**Keywords:** Strong rain, flash floods, terrain position index, runoff simulation, danger estimation

## 1. INTRODUCTION

The UN Report on “Human Costs of Disasters” from 2020<sup>1</sup> compares the development of types of disasters from the decades of 1980 to 1999 with 2000 to 2019 as shown in fig. 1. Most of the disaster types – like e.g. drought, landslides, storms or wildfires – show an increase of about 20 to 50 %. In contrast the increase of flood events stands out with 130 % increase and the largest absolute number of disasters (3254 vs. the second ranked storms with 2043).

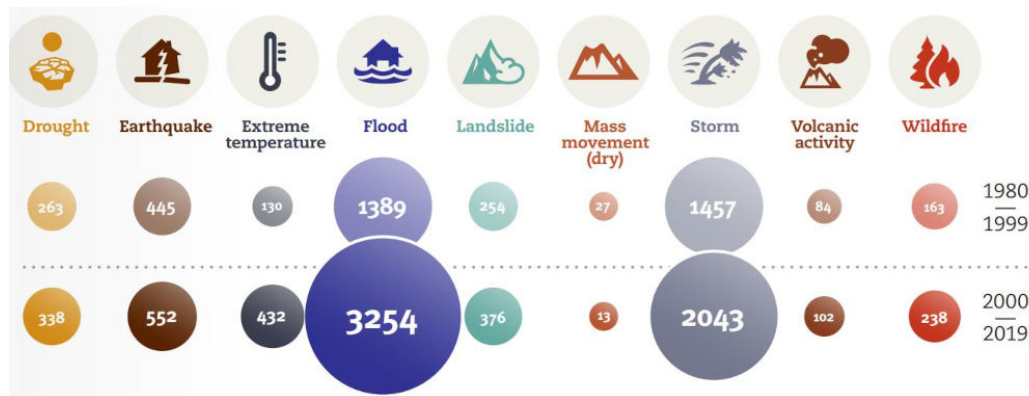


Figure 1. Number of disasters over 20 years by type from the UN report “Human Cost of Disasters”, 2020<sup>1</sup>

Becoming aware of the increasing impact of strong rain events we started already in 2016<sup>2</sup> with the development of methods for danger estimation due to strong rain events. Last year – faced with a occasional flooding event in July 2021 in Germany – we decided to extend our methods also to run-off water from higher areas in narrow valleys. We calibrated and validated the newly developed approaches with aerial imagery acquired shortly after the flooding events and developed a newly combined prediction system for danger estimation due to strong rain events.

In this paper we show how such a combined prediction system can be implemented for the island of Cyprus and compare the resulting flood danger maps with a real flooding event in the vicinity of Nicosia.

Further author information: E-mail: thomas.krauss@dlr.de

## 2. PREVIOUS WORK

### 2.1 Terrain positioning index

As described in 2 a method for deriving a strong rain danger map was developed in cooperation with a German insurance company. The method is based only on a digital elevation model (DEM) of the region of interest. Analyzing the run-off of the local rain in strong-rain conditions shows the low importance of sewage and the drainage system. In this case leaves and branches rapidly block sinks and also the drainage system is mostly not capable to drain off such amounts of water in a short time. Also the natural seepage on pervious ground has in heavy strong rain events no real influence on holding back the flooding water, since dry soil needs some time to start absorbing water.

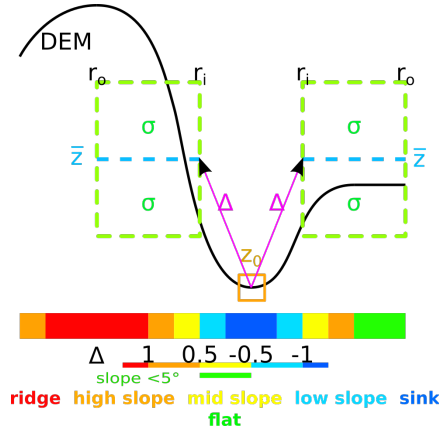


Figure 2. Principle of the calculation of the terrain position index (TPI)

In this research we found that the terrain positioning index (TPI) as presented in 3 and 4 gives the best estimation of endangerment by local strong rain events. The principle of the TPI calculation is shown in fig. 2. This index classifies a DEM based on the relative difference between the elevation of a cell  $z_0$  and the average elevation  $\bar{z}$  of a ring  $R$  ranging from an inner radius  $r_i$  to an outer radius  $r_o$  around the cell:

$$\bar{z} = \frac{1}{N} \sum_{i \in R} z_i \quad \sigma = \sqrt{\frac{1}{N-1} \sum_{i \in R} (z_i - \bar{z})^2} \quad (1)$$

$$\Delta = z_0 - \bar{z} \quad TPI = \frac{\Delta}{\sigma} \quad (2)$$

The TPI is defined relative to the standard deviation of the heights in the ring, not using any absolute height differences. For each point of a DEM in a ring  $R$  ranging from  $r_i$  to  $r_o$  around a DEM point  $z_0$  the mean  $\bar{z}$  and the standard deviation  $\sigma$  is calculated. Based on the relative  $TPI = (z_0 - \bar{z})/\sigma$  the six classes as shown in tab. 1 are derived.

Table 1. Definition of the TPI classes

Class	$TPI$	Slope	Color
ridge	$1 \leq TPI$		red
high slope	$0.5 \leq TPI < 1$		orange
mid slope	$-0.5 \leq TPI < 0.5$	$\geq 5^\circ$	yellow
flat	$-0.5 \leq TPI < 0.5$	$< 5^\circ$	green
low slope	$-1 \leq TPI < -0.5$		cyan
sink	$TPI < -1$		blue

The radii  $r_i$  and  $r_o$  were calibrated and validated using insurance data from a time span of 10 years of an area in North Rhine Westphalia in Germany. Fig. 3 shows the result from this analysis. The blue bars and the right axis show the probability of a household in the class being affected by a strong rain event in 10 years. The red bars related to the left axis show the mean loss of an household of this class in the case of a strong rain event. The numbers above the bars give the total number of households in this class. As can be seen the probability being struck by a strong rain event raises from below 2.5 % in the class “ridge” to 12 % in the class “sink”. The mean loss in such an event raises even from below 100 EUR to over 500 EUR.

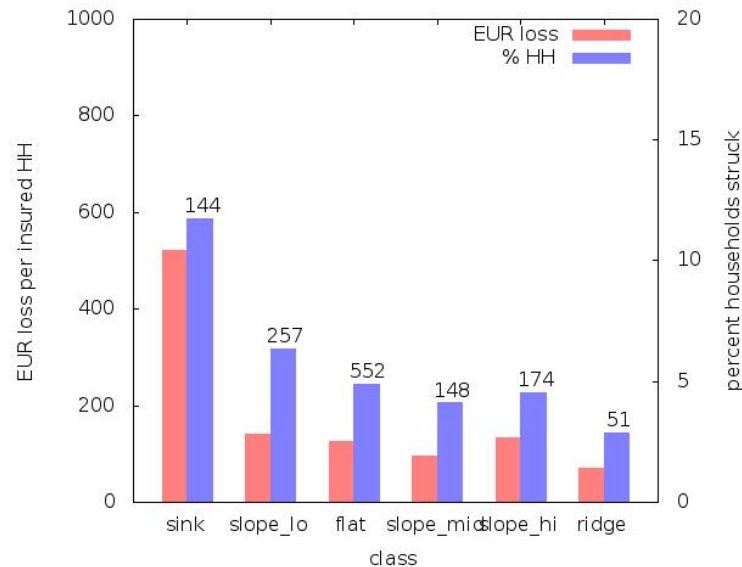


Figure 3. Evaluation of the calibrated danger classes

Based on these results a strong rain danger map for whole Germany and Austria were derived and are used by companies for the rating of real estate.

## 2.2 Run off simulation

In July 2021 a heavy strong rain event occurred at the Ahr river in Germany. Due to the rain covering all of the headwaters of the Ahr a flash flood caused by the narrow valleys occurred in the lower course of the river. This led us to implement a new simulation based on the complete catchment of an area as described in 5.

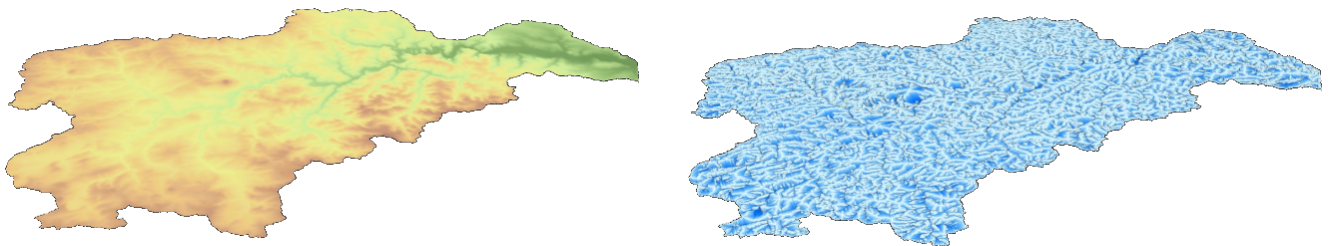


Figure 4. 3D view of the catchment area of the Ahr river in Germany, left: SRTM-DEM, right: runoff-map

The newly developed method is – similar to the method described in 2.1 – based only on a digital elevation model (DEM) not using meteorological, drainage or perviousness information as described above. But now the DEM has to cover the entire catchment of an area to be processed. In a first step, local depressions are filled in the DEM to calculate runoff directions. Based on the runoff direction map, an initial rainfall amount is iteratively

distributed according to these directions and cumulated. The result is a runoff map containing the amount of water flowing through each pixel as shown in fig. 4 (the darker the blue the higher the amount of water flowing through this point).

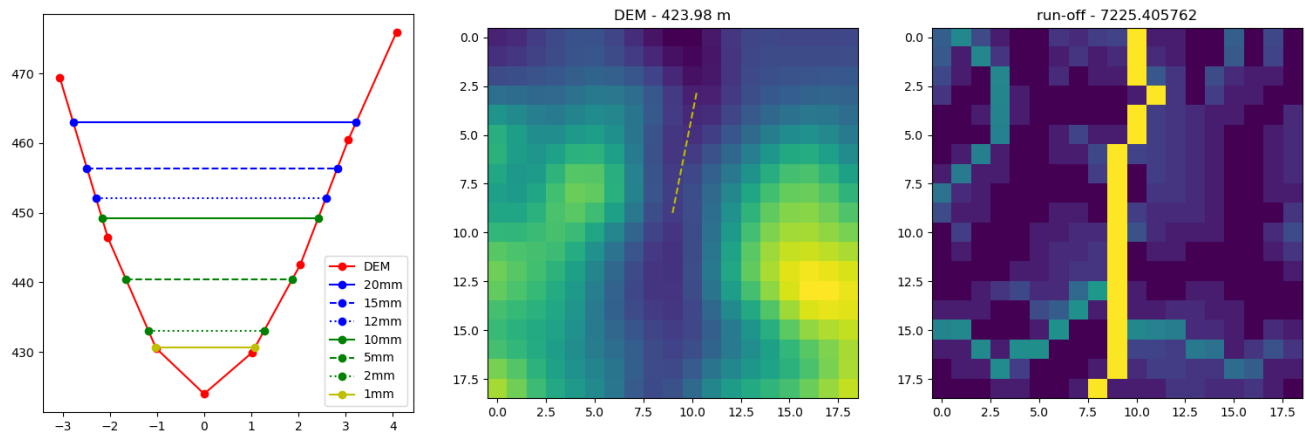


Figure 5. Principle of the fill-level-calculation, left: DEM-profile across runoff-direction with derived fill-levels for different rain volumes over the upstream catchment area, center: DEM with runoff-direction, right: runoff-map

For explanation of the method please refer to fig. 5. In the center a small section of a DEM around the point for which we want to extract the profile is shown together with the derived runoff-direction. Depicted on the right is the corresponding runoff-map. On the left side the extracted profile crossing the point of the DEM across the runoff-direction is shown. The runoff-value 7225 at our point means 7224 pixels are upstream of this point in the runoff-map and contribute to the water-flow through this point. Assuming a rain volume of 1 mm/m<sup>2</sup> over the catchment adds up to 7225 mm/m<sup>2</sup> at this point or – working with pixel sizes – generally also 7225 mm/px or a water column height of 7.225 m in this pixel. Mostly we use different resolutions  $r$  for the DEM and the runoff-map since a smaller runoff-map is calculated much faster. In this case the runoff-values have to be multiplied by  $r_{ro}^2/r_{DEM}^2$  to give the correct runoffs in mm/px in the DEM.

This volume is distributed across the profile as shown in the profile-plot in fig. 5, left, for different rain volumes from 1 to 20 mm/m<sup>2</sup>. In fig. 6, left, a 3D view of a small section of the Ahr runoff-map is shown. Higher values mean higher accumulated water amounts from regions above. In the right bottom area the sinuosity of the Ahr near Ahrbrück can be seen, which is shown in detail in the DEM on the right side.

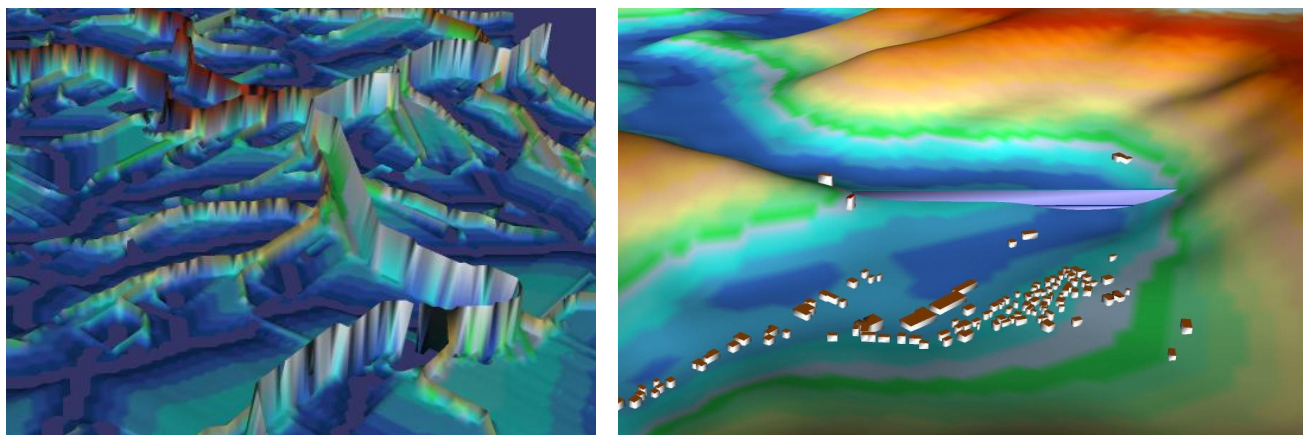


Figure 6. 3D view of the calculated cumulated runoff-map (left), and the DEM of the Ahr-valley near Ahrbrück

Iterating down this runoff-map starting from the highest volume for each “ridge”-point a cross-section in the DEM across the flow direction is derived and filled with the volume given in the runoff-map at that position. The result is a filled profile with water extent and water level height as shown in fig. 6, right. This image shows the DEM and the buildings extracted from OpenStreetMap (OSM). In the bend of the river two light blue “walls” are sketched. These “walls” represent the profiles in the DEM filled up to the given water volume from the runoff-map. The lower profile represents the flood level for a simulated rain amount of  $R_{sim} = 0.05 \text{ mm/m}^2$  over the catchment, the higher the flood level for  $5 \text{ mm/m}^2$ .

Connecting and filling all these derived flood profiles for one simulated amount of rain gives a virtual flood level DEM. Intersecting this with the DEM allows to obtain the flooded areas together with the estimated water levels of the flood.

In 5 this method was developed and the results were calibrated and validated on different areas along the Ahr. For rain amounts over the catchment ranging from  $0.001 \text{ mm/m}^2$  up to  $1.0 \text{ mm/m}^2$  the flooded areas were simulated and compared to the ground truth flooded areas derived from aerial imagery taken shortly after the flooding. For all test areas the intersection over union of the simulated and real flooded areas were calculated. In all areas the best IoU were found for a simulated volume of  $0.05 \text{ mm/m}^2$ .

Actually measured were  $100$  to  $150 \text{ mm/m}^2$  during the strong rain event of 13/14 July 2021. So the derived  $R_{sim}$  value of  $0.05 \text{ mm/m}^2$  corresponds to a measured  $R_{real}$  of  $125 \text{ mm/m}^2$  and thus the resulting calibration for this area is:

$$R_{sim} = \frac{0.05}{125} \cdot R_{real} = 0.0004 \cdot R_{real} \quad (3)$$

### 3. METHOD

Combining the two methods described in 2.1 and 2.2 we create a combined strong rain flood danger map for Cyprus as finally shown in fig. 11. First the catchments of Cyprus were derived from the SRTM<sup>6</sup> as shown in fig. 7.

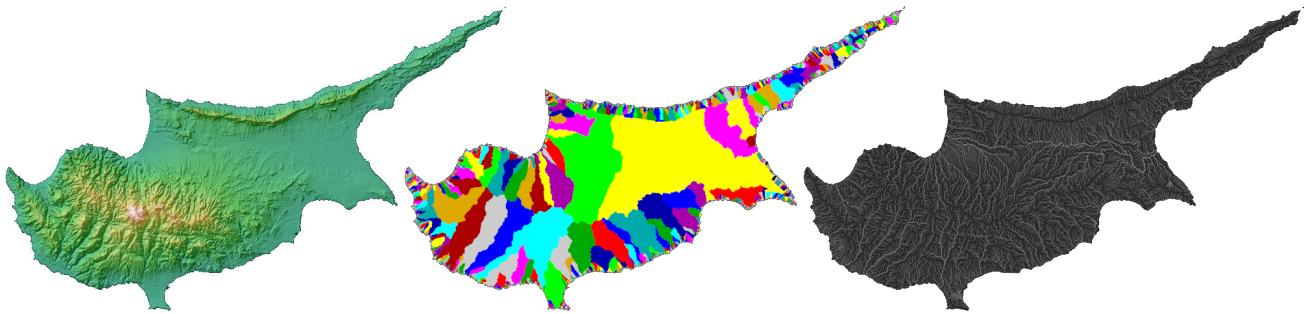


Figure 7. DEM (left), derived catchments (center) and logarithmic scaled runoff-map (right) of Cyprus

Based on the SRTM-DEM a strong rain danger map using the TPI-method as described in 2.1 is calculated. In a second step the flood level DEM based on the runoff map as described in 2.2 is calculated for  $R_{sim}$  values of  $0.01, 0.02, 0.05, 0.1, 0.2, 0.5, 1.0, 2.0, 5.0$  and  $10.0 \text{ mm/m}^2$ .

All of the flood level DEMs with a height of  $10 \text{ cm}$  and more above the DEM are stacked together to create a map of areas which are affected depending on the amount of rain as shown in fig. 8, second from left. Such the flood level map contains values from  $1$  to  $10$  representing flooded areas at  $R_{sim}$  of  $10.0$  down to  $0.01 \text{ mm/m}^2$  with  $10$  representing the highest risk (flooded already in the lowest rain amount) and  $1$  the lowest ( $0$  means no risk detected in the whole stack of flood level DEMs). These values are correlated with the classes from the TPI map and finally a combined strong rain danger map is created (fig. 8, right).

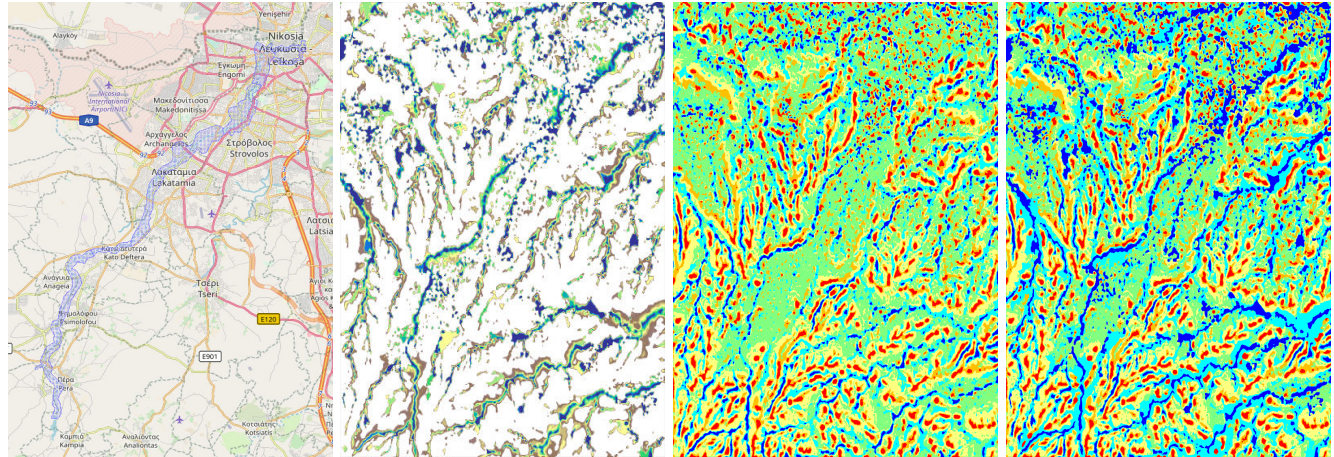


Figure 8. Section covering the Pedaios river ( $20 \times 24 \text{ km}^2$ , from left to right: overview map (OSM), Flood level map, TPI map, combined strong rain danger map

#### 4. EVALUATION

For evaluation we got a flood map from the Pedaios River after a strong rain event on 2003-02-12 with a water level of 169 mm above normal on peak time of 19:55 as shown in figs. 8 and 9 (left). First we calibrated the method described in 2.2 using the available flood map. As shown in fig. 9 (right) we calculated the profiles for different simulated amounts of rain over the upstream catchment of the Pedaios River. This calibration gives a simulated  $R_{sim} = 0.5 \text{ mm/m}^2$  for this flooding event. Since no total amount of rain was available the calibration in eq. 3 could not be validated.

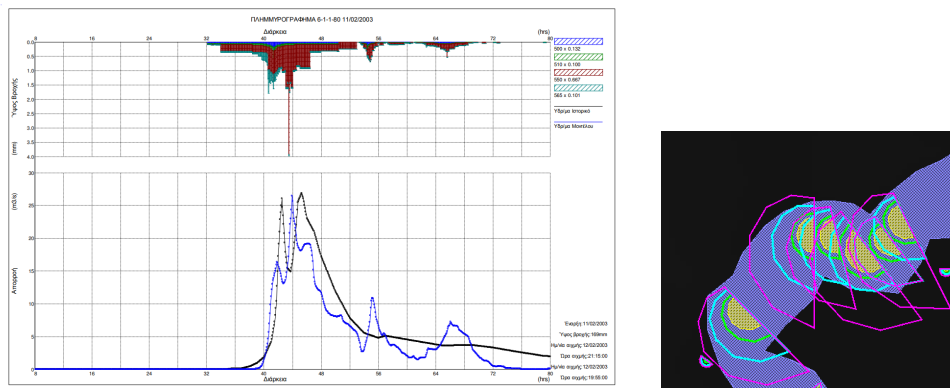


Figure 9. Calibration of runoff values, left: amount of rain on 2003-02-11 to 13 and flood volumes in  $\text{m}^3/\text{s}$ , right: section of the Pedaios river,  $1.3 \times 1.1 \text{ km}^2$ , manually extracted flood-extend (blue) and simulated flood profiles for  $R_{sim}$  of 0.1 (orange), 0.2 (green), 0.5 (cyan) and 1.0 mm (purple) precipitation

The Water Development Department (WDD) gave us the following information on this section of the Pedaios river and this special flooding event:

“This section of the river affected by floods is from Politiko village to the Municipality of Nicosia and covers a distance of 25.3 km. This river is vulnerable to flash flooding. Part of the Pedaios River passes through the Residential Communities/Municipalities of Politikou, Pera, Episkopeio, Ergates, Psimolofou, Aidayia, Devtera, Lakatameia, Engomi, Strovolos, and Nicosia. The banks of the river are under increasing urbanization and population growth, while areas of the flood plain are used as sports grounds, stadiums, parks, etc. A large

number of bridges benefit transportation but not all of them were constructed with a complete hydrologic or hydraulic study. Also, many of these bridges are in the form of Irish Bridges that pose risks. Over the past 150 years, many floods have been recorded of low to very high severity as shown in table 2.

Table 2. Floods of the Pediaios river recorded in the past 150 years

<i>Nr. of floods</i>	<i>severity</i>	<i>T</i>
26	very low	6 years
10	low	15 years
4	moderate	38 years
4	very high	38 years

Some of them also caused deaths. Throughout the river, the riverbed is in the Z3 protection zone, varying in width from 20 to 200 m, (mainly this width is 100 to 120 m). The existence of this Zone reduces the risks of serious flood events and their impact. It is also noted that an enrichment dam has recently been built in the Tamasos area which, through correct operation, may allow a form of large flow management. Since, many of the floods took place long time ago, the information on flooding details is limited.

On 2003-02-12, Strovolos and Lakatamia, areas that form parts of the Pediaios River, were affected by flooding. Specifically, during the flood, a bridge of the Pediaios River in Strovolos was flooded, and a bridge in Lakatamia on Kapodistria Street was destroyed. Also, in Psimolofou, two houses were flooded by the overflowing river on the bridge. The flood event started on 2003-02-12 with a flow height of 169 mm and a peak time of 19:55. The type of event was a flash flood. The damage caused by the flood was only economic (moderate), thus no lives were lost. Also, the severity of the flood was described as very low.”

The area of the destroyed bridge in Lakatamia on Kapodistria Street is shown in detail in fig. 10. The bridge is located left above the center of the image.

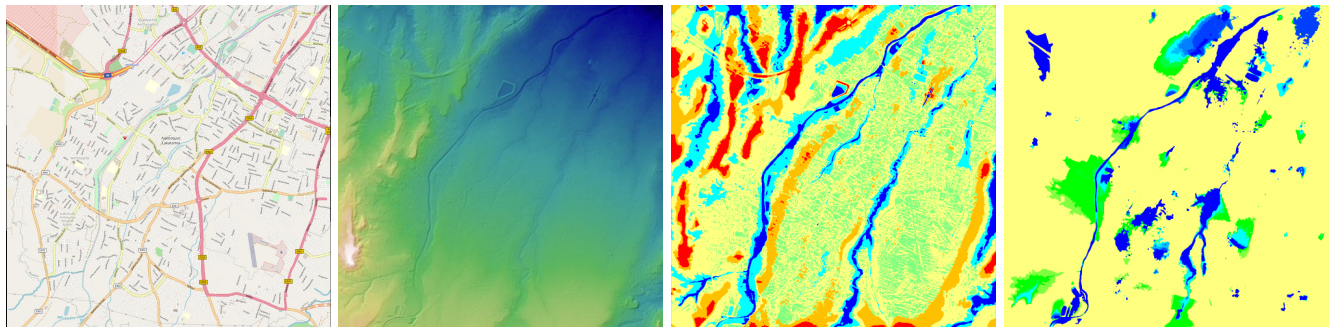


Figure 10. Surrounding of the bridge in Lakatamia on Kapodistria Street which was destroyed,  $5000 \times 5000 \text{ m}^2$ , from left to right: OSM map of the area, 5-m-DEM provided by ECoE, calculated TPI, calculated runoff danger map

As can be seen there are many areas beneath the Pediaios river which are endangered by local effects of strong rain events. The TPI map (second to right in fig. 10) shows these areas. The runoff danger map (fig. 10, rightmost image) adds some more endangered areas caused by flash floods from upstream areas of the river.

## 5. RESULTS

Comparing the different danger maps as shown in fig. 8 with the ground truth flood map from the WDD also shown in fig. 8, left, shows a good estimation using the danger classes “sink” and “low slope” (dark blue and light blue). The new combined danger map (fig. 8, right) adds some more areas prone to flash-floods from upstream areas to these local danger classes.

Finally the resulting strong rain danger map is shown in fig. 11



Figure 11. Final strong rain danger map for the island of Cyprus

## 6. CONCLUSION AND OUTLOOK

In this paper we presented the generation of a combined strong rain danger map for the island of Cyprus which is based on two methods developed at DLR in 2016 and 2022 for estimating the danger of an area to be struck by a flash flood event. A strong rain event as the ones investigated in this and former works show mostly a completely independence of local drainage and perviousness of the surface since the high and rapid amount of water congests drainage systems by branches, leaves or other debris and has no time to seep away. Due to this and assumed total randomness of occurrence of strong rain events we propose two methods for danger estimation based only on the local surface model and the terrain in upstream regions.

The methods were implemented and the map created and validated at one available strong rain event of the Pedaios River. For future work much more strong rain events scattered over the island of Cyprus has to be analyzed and cross-checked with the presented map and probably some parameters – which were derived from strong rain events over Germany – will have to be tuned for Cyprus.

## REFERENCES

- [1] United Nations, “The human cost of disasters: an overview of the last 20 years (2000-2019),” tech. rep. (10 2020).
- [2] Krauß, T. and Fischer, P., “Automatic Detection and Vulnerability Analysis of Areas endangered by Heavy Rain,” in [*Proceedings of European Space Agency, Living Planet Symposium*], *Proceedings of European Space Agency, Living Planet Symposium 2016* (5 2016).
- [3] Weiss, A.-D., “Topographic position and landforms analysis,” *ESRI Users Conference* (2001).
- [4] Zevenbergen, L. and Thorne, C., “Quantitative analysis of land surface topography,” *Earth Surface Processes and Landforms* **12**(2), 47–56 (1987).
- [5] Krauß, T. and Gstaiger, V., “A new Approach to Hazard Analysis of Heavy Rainfall Events based on the Catchment Area of the Ahr River,” in [*ESA Living Planet Symposium 2022*], *ESA Living Planet Symposium 2022* (5 2022).
- [6] “SRTM, Shuttle Radar Topography Mission.” <https://lta.cr.usgs.gov/SRTM1Arc> (2 2017). (accessed 2/2017).